Droplet Open Access

A small droplet, a big world!

Topographies that mantain a constant Wenzel roughness factor over the nanometer to macroscopic vertical range

Journal:	*Droplet*
Manuscript ID	Draft
Wiley - Manuscript type:	Research Article
Date Submitted by the Author:	n/a
Complete List of Authors:	Méndez-Vilas, A.; Formatex Research Center SLU, Director
Keywords:	
Abstract:	The wetting of solid surfaces is directly involved in a large number of important phenomena as lubrication, corrosion, biocompatibility of implants or bacterial adhesion. The surface roughness of the material plays an important role in its interaction with the wetting liquid. One of the parameters used in one of the most used models to analyze the wetting of materials, the Wenzel model, captures the roughness of the material through the so-called Wenzel roughness parameter, which by definition is the ratio between the surface area that develops a rough surface and the one it would have if it were perfectly flat. This model was intuitively developed in 1936 to account for experimental results showing that the wettability of a material increased by imposing roughness. In this brief note we present a characteristic of this parameter, and it is that for a series of topographies structured in the form of periodic patterns of protrusions whose height can vary from the order of nm to macroscopic values, of hemispherical, conical, cylindrical, and pyramidal shapes, this parameter does not show any variation with the height of the same (thereby predicting a null influence of the roughness in the wetting).

Topographies that mantain a constant Wenzel roughness factor over the nanometer to macroscopic vertical range

A. Méndez-Vilas
Formatex Research Center SLU, 06010 Badajoz, Spain
Correspondence: e-mail: amendezvilas@gmail.com; Phone: +34644389624
Personal website: https://scholar.google.es/citations?user=XVejCGYAAAAJ

Abstract

The wetting of solid surfaces is directly involved in a large number of processes as important as the lubrication or corrosion of materials, and indirectly in the biocompatibility of implants or bacterial adhesion, and as such is currently a very active field of research. The surface roughness of the material plays an important role in its interaction with the wetting liquid. One of the parameters used in one of the most used models to analyze the wetting of materials, the Wenzel model, captures the roughness of the material through the so-called Wenzel roughness parameter, which by definition is the ratio between the surface area that develops a rough surface and the one it would have if it were perfectly flat. This model was intuitively developed in 1936 to account for experimental results showing that the wettability of a material increased by imposing roughness. In this brief note we present a characteristic of this parameter, and it is that for a series of topographies structured in the form of periodic patterns of protrusions whose height can vary from the order of nm to macroscopic values, of hemispherical, conical, cylindrical, and pyramidal shapes, this parameter does not show any variation with the height of the same (thereby predicting a null influence of the roughness in the wetting). We present this broad set of topographic designs (to which more can be added) to account for this limitation of the Wenzel roughness factor and contribute to the debate about its applicability and usefulness in the analysis of real-world materials and phenomena.

Keywords: Wetting; Wenzel model; topography; Wenzel roughness factor; AFM

Graphical abstract

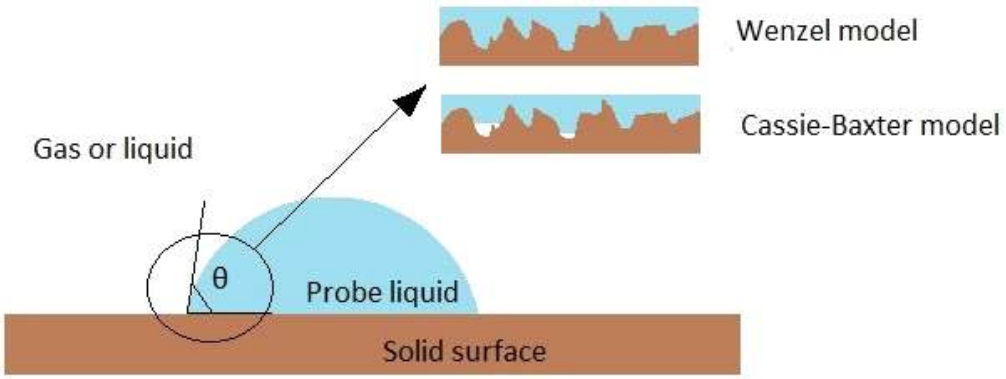

1. Introduction

1.1. Some fundamentals on the Wenzel roughness factor.

The wetting of rough surfaces can be analyzed by several models, the Wenzel and Cassie-Baxter models being the most commonly used. The Wenzel model assumes that the liquid completely wets the irregularities of the material, i.e., it completely penetrates the irregularities, as shown in the Fig. 1. The Cassie-Baxter model assumes that the liquid is suspended not only over the material, but also over pockets of trapped air, thus "seeing" a surface composed of material and air. Both models assume that the average size of the surface irregularities are much smaller than the droplet size, which is generally the case.

Although both models are widely used in the description of surface wetting, a phenomenon involved in a multitude of processes of both scientific and industrial interest, discrepancies between the measured values and those predicted by the theoretical models are frequently published.[1] There is heated debate in the scientific community about the applicability and usefulness of these models, although they are in fact widely applied by a large community ranging from industrial engineers to microbiologists.[2]

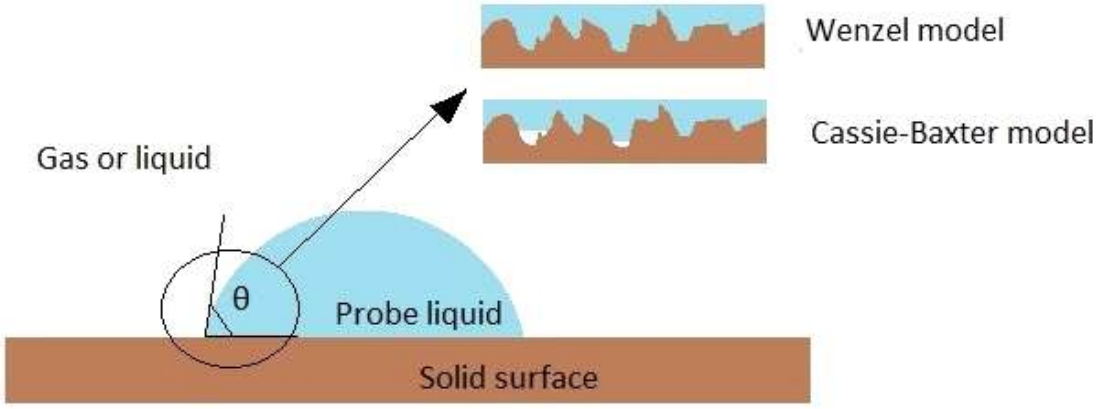

Figure 1. Scheme of the Wenzel and Cassie-Baxter interpretation of the wetting of a solid surface by a liquid drop.

In this note we focus on analyzing one of the features of the Wenzel model. According to this model, proposed by Wenzel in 1936, the modification of the equilibrium contact angle that produces roughness can be modeled using the Wenzel equation, which was proposed intuitively, not formally deduced, in view of experimental results and is shown below[3]:

$$\cos\theta_{rough} = r \cdot \cos\theta_{intrinsic}$$

Equation 1

where

$$r = \frac{A_s}{A_p}$$

Equation 2

In this equation, $\theta_{intrinsic}$ is the intrinsic contact angle of the (smooth) surface, while θ_{rough} is the contact angle on the rough surface. r is the so-called Wenzel roughness parameter, which by definition, is the ratio between the surface area developed by the topographic irregularities (A_s) and the vertically projected area (A_p). r is dimensionless. Evidently, r is always $\geq$ 1, with 1 corresponding to a perfectly (atomically or molecularly) flat surface. If, for example, the imposed roughness increases the surface by 20%, r will take the value 1.2. We can interpret from this equation that roughness amplifies the hydrophilic or hydrophobic character of the surface. That is, it makes an intrinsically hydrophilic surface even more hydrophilic, and a hydrophobic surface even more hydrophobic.

Values of r can be obtained from Equation 1, but in many cases it is not possible to know the $\theta_{intrinsic}$ value (i.e., the material is naturally roughened). Experimental estimates have been obtained with different techniques, such as AFM or Confocal

Microscopy.[4,5]

In practice, materials of interest in science or industry undergo physical or chemical surface conditioning processes. Values of r on commonly used surfaces are between 1 and 2. In general, a value of r greater than 2 is considered to be a very rough surface. To illustrate r with experimental values, we can cite several examples: values in the vicinity of 1.3 were achieved by grit blasting a steel. Much higher values, reaching about 4.5, were achieved by incorporating periodic micrometric irregularities into its surface.[6] Values of up to about 5 were achieved on the polymer by treating it with a femtosecond laser[7]. Values between 1.2-1.5 were measured for a microtextured superhydrophobic silicon surface, and between 1.25-2.10 for a regular untextured aluminum surface (after treatment with a strong acid).[8]

In this short essay, we analyze the Wenzel roughness factor on a set of simple, yet scientifically and technologically relevant, topographical configurations, where it is clearly shown that r need not be an adequate descriptor of surface roughness, since on such surfaces r is practically invariant to changes in what is commonly considered roughness of a material. That is, although it is an experimental fact that a material that has been conferred surface roughness exhibits a different contact angle than the smooth analog, surface roughness is not well determined by r, as we shall see, since we shall show that there are examples of very rough materials that have exactly the same value of r as the less rough counterpart. I present this short essay to contribute to the current debate on the validity of the Wenzel and Cassie-Baxter models in the analysis of wetting phenomena and related phenomena using contact angle values (surface forces, evaluation of Gibbs free energies and their influence on adhesion or adsorption processes...)[9,10.]

1.2. Some fundamentals on the surface roughness of materials.

The most commonly used parameters are the so-called amplitude parameters. They characterize the surface according to the vertical variations of the sample profile. Many of them are closely related to statistical parameters used for sample characterization (arithmetic average, interval amplitude...).[11] We define here the two parameters, easy to compute, that we will use later to get a numerical descriptor of the variations of the height profiles.

$S_{average}$ (height arithmetic average), represents the average of the heights (z_i or $z(x)$ in the continuous case) of all points (N) in the scanned sample area (of length l):

$$S_{average} = \frac{1}{N}\sum_{i=1}^{N} z_i = \frac{1}{l}\int_0^l z(x)dx = \bar{z}$$

Equation 3

It is a value directly proportional to the heights of the surface points, by definition.

R_z (maximum height), represents the height difference between the highest and lowest point within the scanned area.

2. Results and discussion

In this Note, we will analyze geometrically ordered topography surfaces where topographic irregularities take the form of hemispheres, cones, cylinders, and pyramids, being adjacent to each other (Fig. 2). This type of surface structuring can be found both in nature and created by humans ad-hoc for applications or for use in research studies related to topography. In all these cases we will derive the Wenzel roughness factor, r, and see its behavior with the height of the topographic irregularities (commonly referred to as roughness).

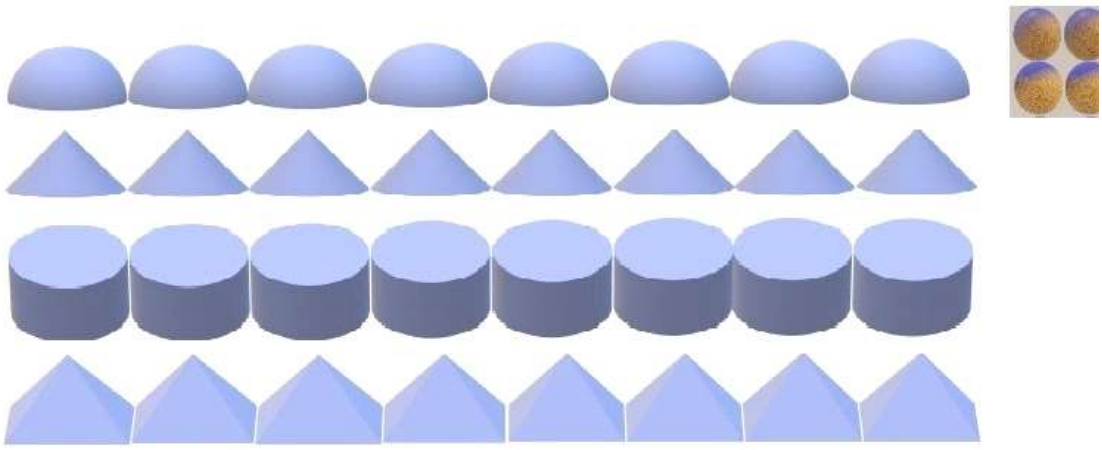

Figure 2. Scheme of the types of ordered topographies that will be shown and analyzed in this Note. The 2D arrangement is shown for the case of the hemispheres, and is the same for the other geometries.

2.1. Ordered pattern of hemispherical protrusions.

Examples of the use of this type of topography can be found in the literature. [12,13] In Fig. 3 we show the geometric characteristics of the elements of this surface.

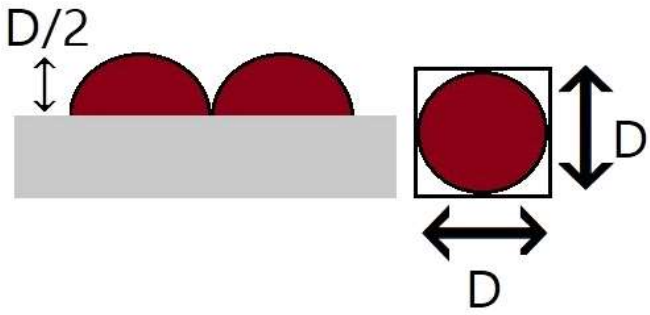

Figure 3. Scheme of the side view and from above the surface, where the dimensions of the hemispheres can be seen.

Consistent with the character of the roughness parameter of r, one expects the roughness parameter to increase with increasing height of the protrusions. That is, a surface texture formed by hemispheres of 10 nm in diameter is a much flatter surface than one formed by hemispheres of 1000 nm (1 um), and this in turn is flatter than one formed by hemispheres of 100,000 nm (100 um). All of them meet the requirement of being much smaller than the capillary length of the liquid, 2.7 mm in the case of water, the maximum size allowed for the drop.

A liquid drop on this surface rests on the upper surface of the hemisphere and on the 4 parts that remain at the vertices of the square. This is the "unit cell" which can be thought of as repeating itself to form the entire structured surface. The area of a hemisphere is $1/2\pi D^2$, if we put it in function of the lateral dimensions of the protrusions (diameter, in this case). The area of the four parts remaining at the vertices can be calculated as: $D^2 - \pi D^2/4$. The total surface area that wets the liquid will therefore be: $A_s = 1/2\pi D^2 + D^2 - \pi D^2/4$. Therefore, the Wenzel roughness factor, r, can be expressed as:

$$r = \frac{A_s}{A_p} = \frac{(\frac{1}{4}\pi+1)D^2}{D^2} = 1.785 \neq f(height\ of\ protrusions, I$$

Equation 6

Interestingly, Wenzel's model predicts the same contact angle whatever the heights of the hemispheres. This is obviously contrary to experience, since experimentally we know that the roughness varies with the amplitude of the irregularities of the material (roughness). This analysis shows that the Wenzel factor does not capture the full essence of the influence of roughness on the equilibrium contact angle of the droplet.

This is illustrated in Fig. 4, where the relative sizes of the hemispherical protrusions could be even more exagerated (always meeting the requirement of being much smaller than the droplet size), since the size variation factor could perfectly be in the environment of 1,000 (from 10 to 10,000 nm, for example) and in the scheme shown in Fig. 4 the variation is in the environment of only 30:

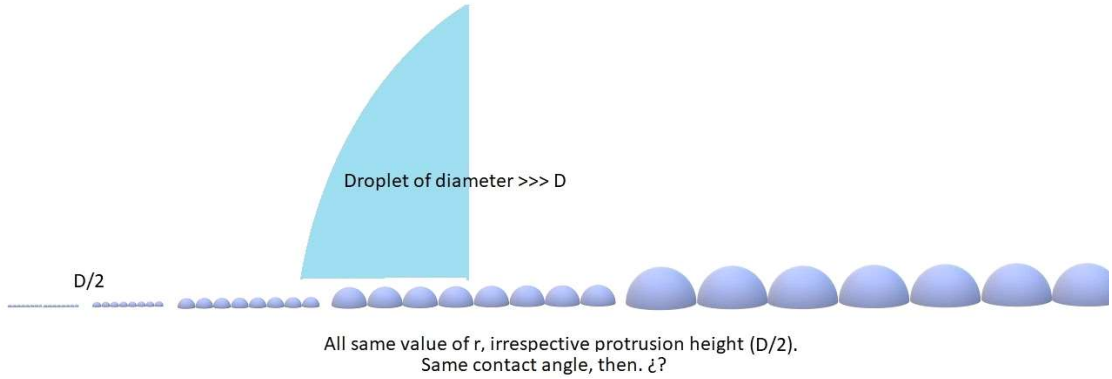

Figure 4. Scheme illustrating the result of computing r in a topography of the ordered pattern type of spheres by varying their dimensions.

This inconsistency in the predictions of the Wenzel model seems to be due to Wenzel's own definition of the roughness parameter. This constancy of the parameter r with the height of the protrusions contrasts with the behavior of other roughness parameters, which do describe the increase in roughness. Let's look at the average height $S_{average}$. In the case of a hemisphere, the average height of its points gives a $S^{average}$ value = 2/3 R, that is, it is proportional to the height of the protrusions (R or D/2). Now, not all the points are on the lateral surface of the hemisphere. There are also height 0 (ground) in the 4 areas adjacent to the vertices. The percentage of points that are on the hemispherical surface with respect to the total is $1/2\pi D^2$ / ($1/4\pi D^2 + D^2$), that is, 88%. The remaining 22% are on the ground. Therefore, the value of $S_{average}$ must be corrected to account for only 88% being on the hemispheres. $S_{average}$, corrected, is $S_{average}$ (corrected) = 0.88 $S_{average}$, which is still proportional to D/2. Also the parameter R_z, which in this case has the value R_z=D/2, is proportional to D.

This type of behavior of the roughness parameters is more consistent with the evidence of being "rougher" (that is, presenting more variations in height) than the behavior of r, which is shown to be constant.

2.2. Orderly pattern of conical protrusions.

Examples of the use of this type of topography can be found in the literature. [14-18] In

Fig. 5 we show the geometric characteristics of the elements of this surface.

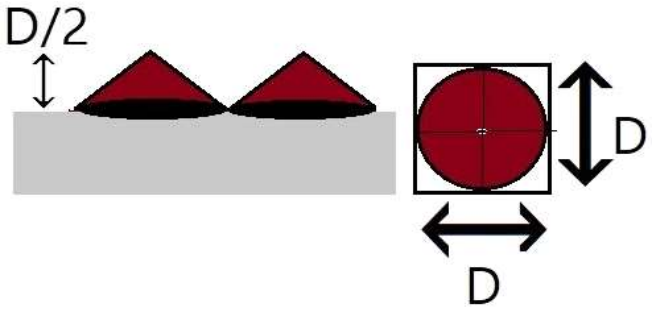

Figure 5. Scheme of the side view and from above the surface, where the dimensions of the cones can be seen.

Now we calculate r for a surface formed by adjacent cones, of height equal to the radius of the base. The lateral area of the cone can be calculated as $A_l = \pi Rg$, where g is the generatrix. In this case, since the height of the cone is equal to the radius, the generatrix is the hypotenuse of a right triangle with legs D/2: $g = D \cdot \sqrt{2}/2$. The total area that wets the liquid will be the sum: $A_s = (\sqrt{2}/4)\pi D^2 + D^2 - \pi D^2/4 = \sqrt{2}\text{-}1/4)\pi D^2 + D^2$. Therefore, the Wenzel roughness factor, r, can be expressed as:

$$r = \frac{A_s}{A_p} = \frac{(\frac{\sqrt{2}-1}{4}\pi+1)D^2}{D^2} = 1.325 \neq f(height\ of\ protrusions,\ l$$

Equation 7

Again, we find a topographic configuration for which the Wenzel model predicts the same value of r and therefore of θ_{rough}, regardless of the height of the topographic irregularities (D/2 or R, in this case).

Regarding the behavior of other roughness parameters, $S_{average}$ (average height of the points) takes the value $S_{average} = D/4$ (the average height of the points of a cone is half its height), that is, it is proportional to the height of the protrusions (D/2). This can be seen by considering Fig. 6. The equation of any of the lines whose revolution around the z axis gives rise to the cone is: $z = h - h/(D/2)\cdot x$. Integrating this equation between the limits 0 and D/2 and dividing by the amplitude of the integration interval (D/2), the average value of the height is obtained, which is $S_{average} = D/4$. Again, you have to correct the value for the points on the ground. In this case there is 84% on the lateral surface ($\sqrt{2}/4)\pi D^2$ / ($\sqrt{2}\text{-}1/4)\pi D^2 + D^2$) and 26% on the ground. Therefore, $S_{average}$ (corrected) = 0.84 $S_{average}$, which is therefore still proportional to D/2. This behavior directly proportional to D is the one expected

since $S_{average}$ has dimensions of length and for D=0 it takes the value 0, the expected value for a perfectly smooth surface. Finally, also the parameter R_z, which in this case has the value R_z=D/2, is proportional (equal) to D/2.

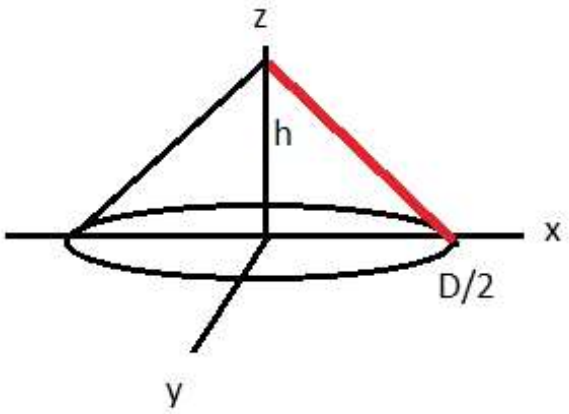

Figure 6. Detail of one of the lines, whose revolution around the z axis gives rise to the cone.

2.3. Orderly pattern of cylindrical protrusions.

Examples of the use of this type of topography can be found in the literature. [19,20] In Fig. 6 we show the geometric characteristics of the elements of this surface.

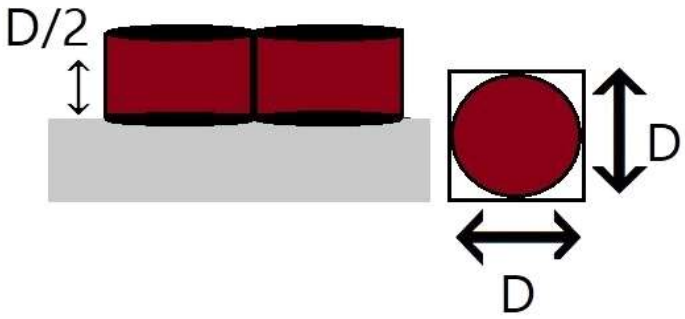

Figure 6. Scheme of the side view and from above the surface, where the dimensions of the cylinders can be seen.

Now we calculate r for a surface formed by adjacent cylinders, of height equal to the radius of the base. The surface area of the cone can be calculated as the sum of the side area plus the area of the top: $A_s = D^2 - (\pi/4)D^2 + (\pi/2)D^2 + (\pi/4)\ D^2 = (1+\pi/2)\ D^2$. Therefore, the Wenzel roughness factor, r, can be expressed as:

$$r = \frac{(1+\frac{\pi}{2})D^2}{D^2} = 1 + \frac{\pi}{2} = 2.571$$

Equation 8

Again, a topographic configuration that gives a value of r independent of the heights

of the protrusions.

Regarding the behavior of other roughness parameters, $S_{average}$ (average height of the points) takes the value $S_{average}$ = D/4 (the average height of the points of a cylinder is half its height), that is, it is proportional to the height of the protrusions (D/2). Again, you have to correct the value for the points on the ground. In this case there is 91.4% on the lateral surface (((π/2)D^2 + (π/4) D^2)/ (D^2 - (π/4)D^2 + (π/2)D^2 + (π/4) D^2)) and 8.6% on the ground. Therefore, $S_{average}$ (corrected) = 0.914 $S_{average}$, which is therefore still proportional to D/2. Also the parameter R_z, which in this case has the value R_z=D/2, is proportional (equal, in this case) to D/2. Both parameters take the value 0 for D = 0, as expected.

2.4. Orderly pattern of square-based pyramidal protrusions.

Examples of the use of this type of topography can be found in the literature. [14,21]. In Fig. 7 we show the geometric characteristics of the elements of this surface.

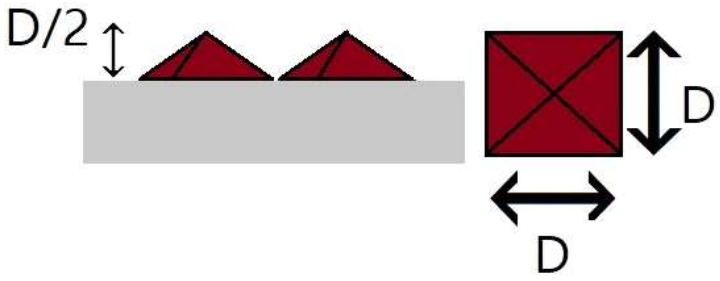

Figure 7. Scheme of the side view and from above the surface, where the dimensions of the pyramids can be seen.

Now we calculate r for a surface formed by adjacent pyramids, of height equal to half the side of the base square (D/2). The lateral area of the pyramid can be calculated as $A_l = P_{base} \cdot Ap$, where P_{base} is the perimeter of the base and Ap is the apothem. In this case, since the height is half the side of the base square, the apothem is the hypotenuse of a right triangle with legs D/2: Ap = $(\sqrt{2}/2)\cdot D$. Therefore, doing simple calculations: $A_l = \sqrt{2}\cdot D^2$. In this case, then, r takes the value:

$$r = \frac{A_s}{A_p} = \frac{\sqrt{2}\,D^2}{D^2} = \sqrt{2} = 1.414$$

Equation 9

Again, we find a topographic configuration for which the Wenzel model predicts the same value of r and therefore of θ_{rough}, regardless of the height of the topographic

irregularities (D/2, in this case).

Regarding the behavior of other roughness parameters, $S_{average}$ (average height of the points) takes the value $S_{average}$ = D/4 (the average height of the points of a pyramid with a square base of height D/2, the demonstration being equal to conical case), that is, it is proportional to the height of the protrusions (D/2). In this case there is 100% of the points are on the pyramid surface, so it is not necessary to correct $S_{average}$. Finally, also the parameter R_z, which in this case has the value R_z=D/2, shows an increasing value, proportional (equal), to D/2. Again, both parameters take the value 0 for D = 0, as expected.

3. Conclusions

We have theoretically constructed and analysed a wide set of not especially complex topographies for which the Wenzel model predicts an invariance of the equilibrium contact angle with the height of the topographic protrusions (invariance of the Wenzel roughness factor), a fact that contradicts the experimental evidence. This characteristic of the Wenzel model, a consequence of the definition of the Wenzel roughness factor, may be interesting to shed light on its applicability, usefulness, and the reasons for discrepancies between what is theoretically predicted and what is obtained experimentally in the scientific community that uses this phenomenon, either as a direct objective of study, or as a basis for understanding other phenomena related to it.

4. Acknowledgments

I would like to thank my former colleagues from the Research Group on Biosurfaces and Interfacial Phenomena of the University of Extremadura (UEX), especially its Director Prof. González-Martín, for how much I learned on the subject of this note in the years I spent doing experimental research there.

References

[1] Mądry, K., Nowicki, W. Wetting between Cassie–Baxter and Wenzel regimes: a cellular model approach. *Eur. Phys. J.* E 44, 138 (2021).

[2] Werb, M., Falcón García, C., Bach, N.C. et al. Surface topology affects wetting behavior of Bacillus subtilis biofilms. npj *Biofilms Microbiomes* 3, 11 (2017).

[3] Wenzel, R.W. Resistance of Solid Surfaces to Wetting by Water. *Industrial and Engineering Chemistry,* 1936, 28, 988-994.

[4] P.J. Ramón-Torregrosa, M.A. Rodríguez-Valverde, A. Amirfazli, M.A. Cabrerizo-Vílchez. Factors affecting the measurement of roughness factor of surfaces and its implications for wetting studies. *Colloids and Surfaces A: Physicochemical and Engineering Aspects,* 1–3, 2008, 83-93.

[5] A. Tsigarida, E.Tsampali, A.A. Konstantinidis, M. Stefanidou. On the use of confocal microscopy for calculating the surface microroughness and the respective hydrophobic properties of marble specimens. *Journal of Building Engineering*, 33, 101876, 2021.

[6] C.M.H. Hagen, A. Hognestad, O.Ø. Knudsen, K. Sørby. The effect of surface roughness on corrosion resistance of machined and epoxy coated steel, *Progress in Organic Coatings* 130:17-23.

[7] L. He, D.F. Farson. Wettability modification of electrospun poly(ε-caprolactone) fiber by femtosecond laser irradiation. *Journal of Laser Applications* 25, 012002 (2013).

[8] Hongru A., Xiangqin L., Shuyan S., Ying Z., Tianqing L. Measurement of Wenzel roughness factor by laser scanning confocal microscopy. *RSC Adv*. 2017;7:7052–7059.

[9] A. Stocco, H.Möhwald. The Influence of Long-Range Surface Forces on the Contact Angle of Nanometric Droplets and Bubbles, Langmuir 2015, 31, 43, 11835–11841.

[10] A.Pietak, S.Korte, E.Tan, A.Downard, M.P. Staiger. Atomic force microscopy characterization of the surface wettability of natural fibres. *Applied Surface Science*, 253, 2007, 3627-3635.

[11] How to select the most relevant 3D roughness parameters of a surface. R. Deltombe, K.J. Kubiak, M Bigerelle. *Scanning* 2014 36(1):150-60.

[12] Q. Gao, J. Li, C. Ding, J. Wang, Z. Chen, X. Yang, In situ real-time investigation of Staphylococcus aureus on hemisphere-patterned polyurethane films. *Colloids and Surfaces B: Biointerfaces*, 216, 2022,112577.

[13] Zhao X, Wen J, Li L, Wang Y, Wang D, Chen L, Zhang Y and Du Y 2019 Architecture design and applications of nanopatterned arrays based on colloidal lithography *J. Appl. Phys*. 126 141101.

[14] V. Malheiro, F. Lehner, V. Dinca, P. Hoffmann and K. Maniura-Weber. Convex and concave micro-structured silicone controls the shape, but not the polarization state of human macrophages, *Biomater. Sci*., 2016, 4, 1562.

[15] L. Wang, F. Zhao, S. Tang, H. Zhao, Z. Liu. Optimal design of micro-topography on natural leaf surface. *AIP Advances* 2021, 11 (9) , 095019.

[16] Y. Wang, J. Deng, J. Duan, B. Zhang. Conical Microstructure Flexible High-Sensitivity Sensing Unit Adopting Chemical Corrosion, *Sensors* 2020, 20(16), 4613.

[17] Z. Tang, P. Wang, B. Xu, L. Meng, L. Jiang, H. Liu. Bioinspired Robust Water Repellency in High Humidity by Micro-meter-Scaled Conical Fibers: Toward a Long-Time Underwater Aerobic Reaction, *J. Am. Chem. Soc*. 2022, 144, 24, 10950–10957.

[18] Cao, W., Alsharif, N., Huang, Z. et al. Massively parallel cantilever-free atomic force microscopy. *Nat Commun* 12, 393 (2021).

[19] Santoro, F., Zhao, W., Joubert, L. M., Duan, L., Schnitker, J., van de Burgt, Y., Lou, H. Y., Liu, B., Salleo, A., Cui, L., Cui, Y., & Cui, B. (2017). Revealing the Cell-Material Interface with Nanometer Resolution by Focused Ion Beam/Scanning Electron Microscopy. *ACS Nano*, 11(8), 8320-8328.

[20] Lin, J., Xu, Y., Fang, Z. et al. Fabrication of high-Q lithium niobate microresonators using femtosecond laser micromachining. *Sci Rep* 5, 8072 (2015).

[21] Filipponi L, Livingston P, Kašpar O, Tokárová V, Nicolau DV. Protein patterning by microcontact printing using pyramidal PDMS stamps. *Biomed Microdevices*. 2016 Feb;18(1):9. doi: 10.1007/s10544-016-0036-4.